Since January 2020 Elsevier has created a COVID-19 resource centre with free information in English and Mandarin on the novel coronavirus COVID-19. The COVID-19 resource centre is hosted on Elsevier Connect, the company's public news and information website.

Antiviral Research 203 (2022) 105329

Contents lists available at ScienceDirect

Antiviral Research

journal homepage: www.elsevier.com/locate/antiviral

Intravenous delivery of GS-441524 is efficacious in the African green monkey model of SARS-CoV-2 infection

Jared Pitts [a], Darius Babusis [a], Meghan S. Vermillion [b], Raju Subramanian [a], Kim Barrett [a], Diane Lye [a], Bin Ma [a], Xiaofeng Zhao [a], Nicholas Riola [a], Xuping Xie [c], Adriana Kajon [b], Xianghan Lu [a], Roy Bannister [a], Pei-Yong Shi [c], Maria Toteva [a], Danielle P. Porter [a], Bill J. Smith [a], Tomas Cihlar [a], Richard Mackman [a], John P. Bilello [a,*]

[a] Gilead Sciences, 333 Lakeside Drive, Foster City, CA, 94404, USA
[b] Lovelace Biomedical Research Institute, 2425 Ridgecrest Drive, SE, Albuquerque, NM, 87108, USA
[c] University of Texas Medical Branch – Department of Biochemistry and Molecular Biology, Galveston, TX, 94070, USA

ARTICLE INFO

Keywords:
SARS-CoV-2
GS-441524
Remdesivir
African green monkey

ABSTRACT

Severe acute respiratory syndrome coronavirus 2 (SARS-CoV-2), the causative agent of the COVID-19 pandemic, has infected over 260 million people over the past 2 years. Remdesivir (RDV, VEKLURY®) is currently the only antiviral therapy fully approved by the FDA for the treatment of COVID-19. The parent nucleoside of RDV, GS-441524, exhibits antiviral activity against numerous respiratory viruses including SARS-CoV-2, although at reduced *in vitro* potency compared to RDV in most assays. Here we find in both human alveolar and bronchial primary cells, GS-441524 is metabolized to the pharmacologically active GS-441524 triphosphate (TP) less efficiently than RDV, which correlates with a lower *in vitro* SARS-CoV-2 antiviral activity. *In vivo*, African green monkeys (AGM) orally dosed with GS-441524 yielded low plasma levels due to limited oral bioavailability of <10%. When GS-441524 was delivered via intravenous (IV) administration, although plasma concentrations of GS-441524 were significantly higher, lung TP levels were lower than observed from IV RDV. To determine the required systemic exposure of GS-441524 associated with *in vivo* antiviral efficacy, SARS-CoV-2 infected AGMs were treated with a once-daily IV dose of either 7.5 or 20 mg/kg GS-441524 or IV RDV for 5 days and compared to vehicle control. Despite the reduced lung TP formation compared to IV dosing of RDV, daily treatment with IV GS-441524 resulted in dose-dependent efficacy, with the 20 mg/kg GS-441524 treatment resulting in significant reductions of SARS-CoV-2 replication in the lower respiratory tract of infected animals. These findings demonstrate the *in vivo* SARS-CoV-2 antiviral efficacy of GS-441524 and support evaluation of its orally bioavailable prodrugs as potential therapies for COVID-19.

1. Introduction

The *Coronaviridae* family is made up of large (~30 kb) positive-sense, single stranded RNA viruses which can infect a wide array of vertebrate species. Humans are susceptible to infection by several coronaviruses (CoVs), from common cold causing CoVs (e.g. OC43, 229E) to those which can cause life-threatening respiratory disease, such as Middle Eastern respiratory syndrome coronavirus (MERS-CoV) and the severe acute respiratory syndrome coronaviruses, SARS-CoV and SARS-CoV-2 (the causative agent of coronavirus disease 2019 (COVID-19)). SARS-CoV-2 emerged in late 2019 and within months, the SARS-CoV-2 outbreak was declared a pandemic by the World Health Organization (WHO). As of December 2021, SARS-CoV-2 has infected more than 260 million people resulting in over 5 million deaths. Additional zoonotic CoVs have the potential to infect human cells (Menachery et al., 2016; Sheahan et al., 2008), indicating future CoV outbreaks are likely to remain a global public health concern.

Remdesivir (RDV, VEKLURY®) is an FDA approved nucleotide prodrug analog indicated for adult and pediatric patients for the treatment of COVID-19 requiring hospitalization. RDV is intracellularly metabolized by the cellular hydrolases, cathepsin A (CatA) and carboxylesterase 1 (CES1), to an alanine metabolite and then to the monophosphate

* Corresponding author.
E-mail address: John.Bilello@gilead.com (J.P. Bilello).

https://doi.org/10.1016/j.antiviral.2022.105329
Received 14 January 2022; Received in revised form 26 April 2022; Accepted 29 April 2022
Available online 5 May 2022

intermediate by the HINT1 phosphoramidase (Li et al., 2021a; Pruijssers et al., 2020) (Fig. 1). The monophosphate intermediate is then rapidly converted by cellular kinases to the pharmacologically active triphosphate (TP, Fig. 1) that inhibits nascent SARS-CoV-2 transcription by the viral polymerase (Gordon et al., 2020; Kokic et al., 2021; Tchesnokov et al., 2020). GS-441524 is the parent nucleoside of RDV and is intracellularly metabolized to the same monophosphate intermediate and subsequently to the active triphosphate (Fig. 1). However, the metabolic pathway of GS-441524 to the monophosphate intermediate is less efficient, resulting in lower cellular SARS-CoV-2 antiviral activity for GS-441524 in comparison with RDV in lung cells (Pruijssers et al., 2020; Xie et al., 2020).

In vivo pharmacokinetic (PK) studies following IV RDV administration in African green monkeys (AGM) and cynomolgus monkeys as well as in rodents have shown a short plasma half-life (0.4–0.8 h) for RDV, however, high levels of the active triphosphate are still detected in lung tissue at 24 h post infusion when plasma RDV is undetectable (Mackman et al., 2021; Sheahan et al., 2017). Conversely, IV administration of GS-441524 results in high and more durable systemic exposure, yet lung TP levels are substantially lower at 24 h post infusion compared to those from a lower molar-equivalent dose of RDV (Mackman et al., 2021; Xie and Wang, 2021). The lower lung TP levels from even high systemic exposure of GS-441524 is presumably due to its lower permeability and limited conversion to the monophosphate intermediate, consistent with *in vitro* observations (Li et al., 2021a; Van Rompay et al., 2000). Despite the lower *in vitro* antiviral efficacy and less efficient *in vitro* and *in vivo* metabolism of GS-441524 compared to RDV, several recent studies suggest high plasma exposures of GS-441524 may be sufficient to overcome the metabolic limitations and demonstrate coronavirus antiviral efficacy *in vivo*. First, in a transgenic mouse model of SARS-CoV-2 infection, treatment with GS-441524 prevented animals from disease-related weight loss and reduced infectious viral loads by nearly 2 $\log_{10}$ in the lung at day 2 post-infection (Li et al., 2021b). Second, the orally bioavailable tri-ester prodrug, GS-621763, which yields high plasma exposures to GS-441524, displayed antiviral efficacy against SARS-CoV-2 in both mouse and ferret models (Cox et al., 2021; Schafer et al., 2022). Finally, in a non-respiratory coronavirus infection model with feline infectious peritonitis virus (FIPV), cats treated with GS-441524 survived the normally lethal disease (Murphy et al., 2018; Pedersen et al., 2019). Taken together, results from these models highlight the potential *in vivo* antiviral efficacy of GS-441524. Here we sought to study both RDV and GS-441524 in a non-human primate model of SARS-CoV-2 to establish GS-441524 systemic levels required for *in vivo* antiviral efficacy. Due to low oral bioavailability of GS-441524 in non-human primates, the IV route of administration was used. In this study, we report the first comparative pharmacokinetics, biodistribution, and SARS-CoV-2 efficacy of IV delivered RDV or GS-441524 in AGM. The cumulative data support further exploration of GS-441524 oral prodrugs for the treatment of COVID-19.

2. Results

2.1. SARS-CoV-2 antiviral potency and metabolism of GS-441524 and RDV in human primary lung cells

We first sought to determine the *in vitro* antiviral potency of GS-441524 and RDV against a SARS-CoV-2 reporter virus containing the firefly luciferase (Fluc) gene in human primary EpiAlveolar cells (differentiated Alveolar Type I and Type II cells in a 3D culture) and normal bronchial epithelial cells (NHBE). In EpiAlveolar culture, Fluc signal at 72 h post-infection had a mean signal above 5 $\log_{10}$ relative light units (RLUs) in the DMSO control and at low compound concentrations (Fig. 2A). Luciferase signals decreased in a dose dependent manner for both GS-441524 and RDV; however, approximately 20-fold

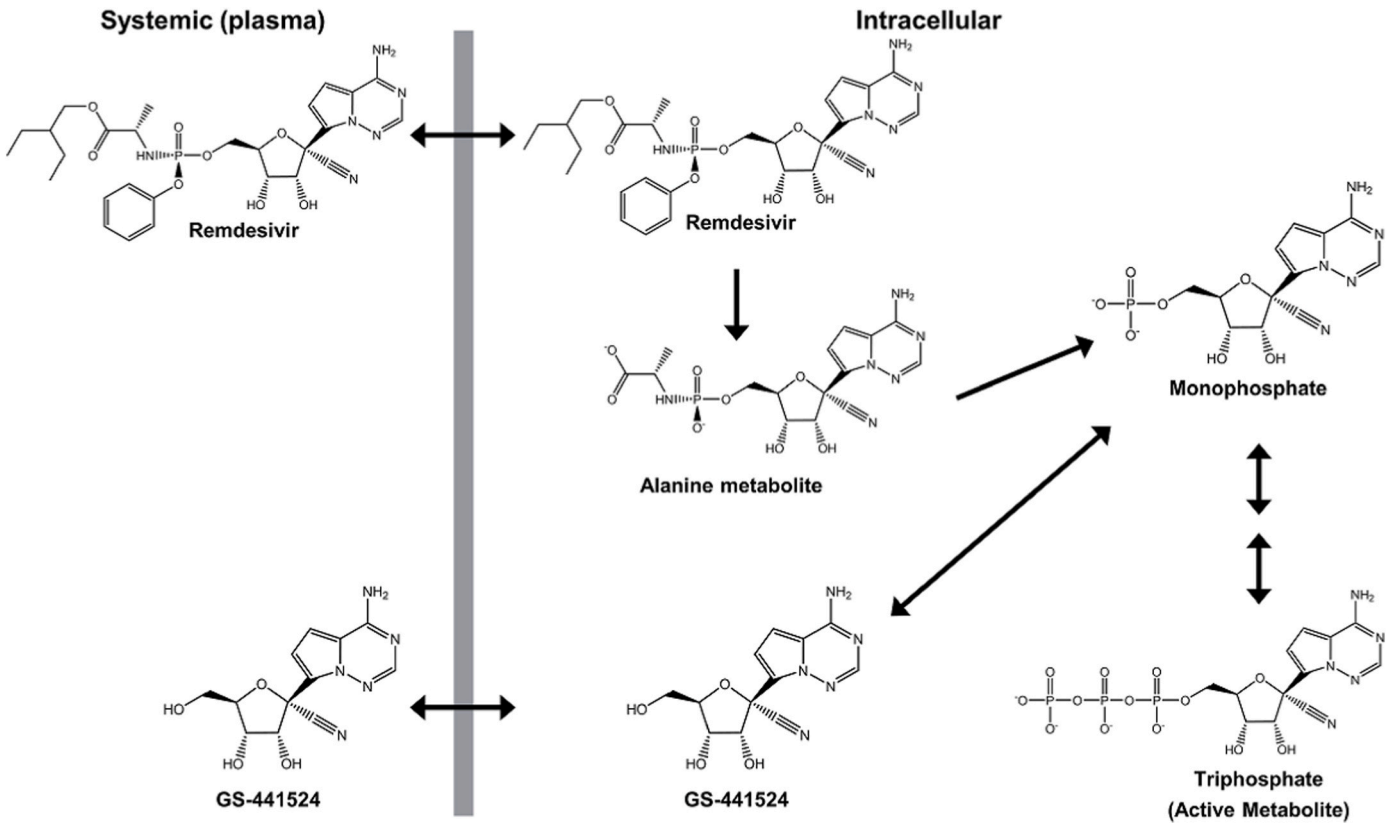

Fig. 1. Remdesivir intracellular and systemic metabolites. Metabolic pathway of intracellular and systemic (plasma) remdesivir and its metabolites leading to the pharmacologically active triphosphate of parent nucleoside GS-441524.

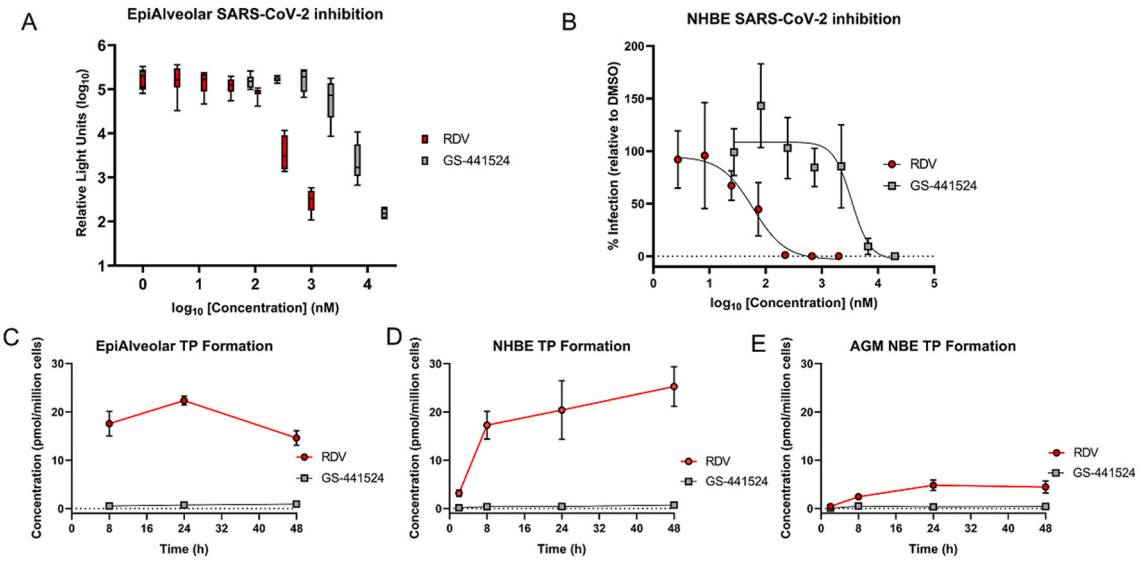

Fig. 2. ***In vitro*** **SARS-CoV-2 antiviral activity and metabolism.** Antiviral activity of RDV and GS-441524 against recombinant SARS-CoV-2 Fluc reporter virus shown with means and standard deviation shown from infected EpiAlveolar cultures 72 h post-infection (A) or NHBE cultures at 24 h post-infection (B). Levels of active triphosphate (TP), sampled during 48 h of continuous incubation with either 1 μM RDV or GS-441524 in EpiAlveolar cells (C) normal human bronchial epithelial (NHBE cells) (D) or AGM normal bronchial epithelial (NBE) cells (E).

higher concentrations of GS-441524 were required to achieve similar reductions in luciferase signal to those achieved with RDV (Fig. 2A). Similarly, in NHBE cells, the half-maximal effective concentration (EC_{50}) values of GS-441524 and RDV were 3400 nM and 37.2 nM, respectively (Fig. 2B, Table 1). The difference in antiviral potency between GS-441524 and RDV in EpiAlveolar and NHBE cells is consistent with other cell lines previously analyzed (Pruijssers et al., 2020; Xie et al., 2020; Mackman et al., 2021). The lower potency of GS-441524 in these two primary lung cell cultures is likely due to decreased metabolic efficiency of GS-441524 conversion to the active TP. To confirm the lower TP levels by GS-441524 compared to RDV, we harvested EpiAlveolar or NHBE cultures at multiple timepoints (2–48 h) after continuous incubation with either compound at 1 μM. The average TP levels over the course of the 48-h incubation were 0.64 and 0.44 pmol TP/million cells for GS-441524 and 15.8 and 19 pmol TP/million cells for RDV in EpiAlveolar and NHBE cells, respectively (Fig. 2C and D, Table 1). Thus, TP levels in these primary human lung cells were 25 to 43-fold lower after treatment with GS-441524 than RDV, which is in line with the lower comparative antiviral potency of GS-441524. The metabolism results from the NHBE donor used in these studies are highly consistent to those previously reported with a different donor (Mackman et al., 2021). These findings further support the correlation between TP formation and SARS-CoV-2 antiviral activity, and that the lower potency of GS-441524 is due to its inefficient TP formation relative to RDV.

As the *in vivo* efficacy of GS-441524 and RDV would be evaluated in SARS-CoV-2 infected AGMs, we also determined the metabolism in primary AGM bronchial cells. Continuous incubation of AGM bronchial epithelial cells with 1 μM of either GS-441524 or RDV resulted 0.32 and 3.7 pmol TP/million cells, respectively (an 11.5-fold difference) (Fig. 2E, Table 1). While the levels of TP were similar following incubation with GS-441524 in either AGM or human bronchial epithelial cells, the TP level observed from RDV incubations was approximately 5-fold lower in cells from AGM relative to human. Nonetheless, these findings show that GS-441524 metabolism to the active triphosphate is consistently less efficient compared to RDV in both AGM and human bronchial epithelial cultures.

2.2. *Pharmacokinetics following either IV GS-441524 or RDV or oral GS-441524 in AGM*

To facilitate *in vivo* studies, we next compared RDV and GS-441524 pharmacokinetics after IV administration of the compounds in healthy AGMs. IV infusions were delivered at a constant rate over 30 min resulting in final doses of 10 mg/kg RDV or 20 mg/kg GS-441524. Following RDV infusion, both RDV and its alanine metabolite rapidly appeared and then declined from plasma, with a mean terminal elimination half-life of approximately 1 h (Fig. 3A), consistent with observations in humans (Humeniuk et al., 2020). In contrast, after RDV administration, GS-441524 appeared in plasma slowly, at lower concentrations than RDV or its alanine metabolite and persisted above detectable levels throughout the 24-h sampling period (Fig. 3A) with a longer mean terminal elimination half-life of over 6 h.

Following IV infusion of GS-441524 at 20 mg/kg, maximal concentrations (C_{max}) of GS-441524 in plasma were approximately 70-fold higher than those observed after a 10 mg/kg RDV infusion and declined with a mean terminal elimination half-life of less than 5 h (Fig. 3A). The GS-441524 plasma exposure following a 20 mg/kg IV administration of GS-441524 was 147 μM·h (Table 2), an 18-fold increase compared to GS-441524 exposure resulting from RDV at 10 mg/kg (Mackman et al., 2021). At 24 h post-infusion, the levels of triphosphate observed in the lower lung tissue were 4-fold lower following administration of GS-441524 compared to RDV (Fig. 3B). These results

Table 1
Antiviral potency and TP levels in primary lung cultures after GS-441524 and RDV treatments.

	SARS-CoV-2 Fluc EC_{50} (nM)	Average TP (pmol/M cells) over 48 h; N = 4-6		
Cell type	NHBE	NHBE	EpiAlveolar	AGM Bronchial
GS-441524	3400	0.44	0.64	0.32
RDV	37.2	19.0	15.8	3.7

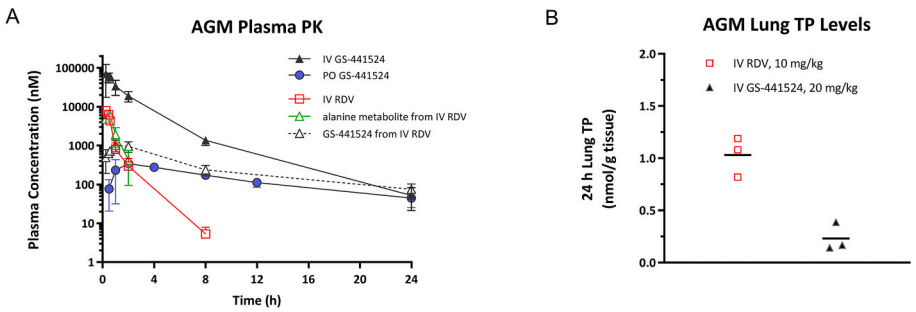

Fig. 3. *In vivo* pharmacokinetics (PK) following GS-441524 or RDV administration in African green monkeys (AGM). (A) GS-441524 plasma PK following intravenous infusion (IV – black triangle) or oral (PO – blue circle) GS-441524 or IV RDV (white triangle) administration. RDV (red square) and the alanine metabolite (green triangle) plasma concentrations after IV infusion of RDV were also monitored. (B) Lung triphosphate (TP) at 24 h post infusion following either 10 mg/kg IV RDV (red square) or 20 mg/kg IV GS-441524 (black triangle) administration.

Table 2
Mean plasma pharmacokinetic parameters following either GS-441524 or RDV administration in AGM.

Test Article	GS-441524		RDV		
Route	IV	Oral	IV		
Dose (mg/kg)	20	5		10	
Analyte	GS-441524		RDV	alanine metabolite	GS-441524
$t_{1/2}$ (h)	2.63 ± 0.19	6.65 ± 1.82	0.77 ± 0.03	0.34 ± 0.05	6.18 ± 0.83
T_{max} (h)	0.47 ± 0.19	1.67 ± 0.58	0.48 ± 0.00	0.33 ± 0.13	1.67 ± 0.58
C_{max} (μM)	87.3 ± 37.4	0.36 ± 0.05	12.6 ± 1.0	15.9 ± 4.9	1.23 ± 0.36
AUC_{last} (μM·h)	147 ± 36	3.15 ± 0.94	7.88 ± 0.96	7.75 ± 1.62	9.06 ± 2.61
AUC_{inf} (μM·h)	147 ± 36	3.69 ± 0.96	7.88 ± 0.96	8.00 ± 1.81	9.82 ± 2.92
F (%)	–	10.0 ± 2.1		–	
Lung TP (nmol/g)	0.23 ± 0.13	NA		1.03 ± 0.19	

are consistent with previous findings in cynomolgus monkeys (Mackman et al., 2021) and demonstrate that when administered itself or as the sole circulating species, GS-441524 requires high exposures in order to achieve similar lung TP levels to those derived from RDV administration.

To determine if the oral route of administration could be used for delivery of GS-441524 in non-human primates, we also investigated the pharmacokinetics of orally administered GS-441524 at 5 mg/kg (Table 2). The oral exposure and the resultant bioavailability of GS-441524 in AGM was low (mean oral F = 10%), consistent with previous findings in cynomolgus monkey (mean oral F = 5% (Mackman et al., 2021)). This led us to pursue a proof of principle efficacy study for GS-441524 in the AGM using IV infusion as the most efficient way to achieve the desired high plasma exposures of GS-441524.

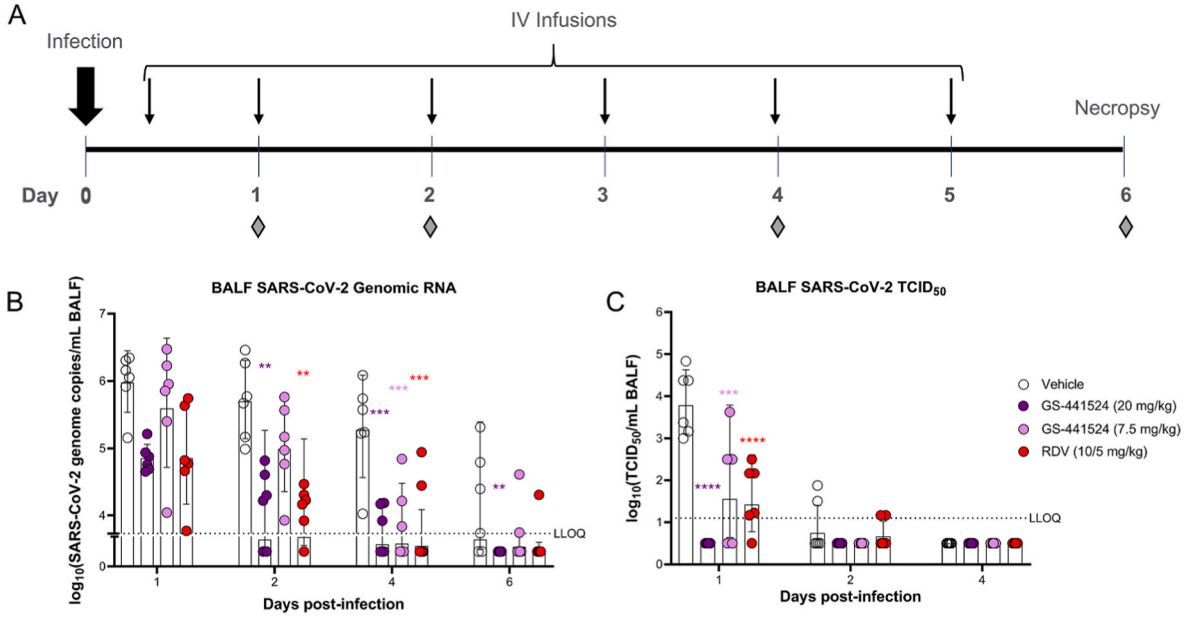

Fig. 4. GS-441524 and RDV reduce SARS-CoV-2 genomic copies and infectious virus in BALF. (A) Schematic of AGM efficacy study with timing of GS-441524 or RDV IV infusions (arrows) and sample collections (grey diamonds) depicted relative to timing of infection at day 0. AGM (n = 6/group) were inoculated with SARS-CoV-2. IV treatment groups included GS-441524 at 20 mg/kg (dark purple symbols) or 7.5 mg/kg (light purple symbols), with RDV at a 10/5 mg/kg regimen (red symbols), or vehicle (open symbols). SARS-CoV-2 genomic RNA copies (**B**) and infectious virus (**C**) were quantified from BALF. Genomic RNA copies were quantified by RT-qPCR and infectious SARS-CoV-2 titers were determined by the $TCID_{50}$ assay. Samples below the lower limit of quantification (LLOQ, dotted lines) for the assay were assigned a value of 1/2 LLOQ for analyses. Statistical analyses were performed using repeated measures two-way ANOVA with Bonferroni post-hoc correction, with $p < 0.05$ being considered significant $^{**}p < 0.01$, $^{***}p < 0.001$, $^{****}p < 0.0001$.

2.3. Efficacy of IV administered GS-441524 and RDV in an AGM SARS-CoV-2 infection model

It has previously been reported that AGMs are a semi-permissive non-human primate model for SARS-CoV-2 infection (Cross et al., 2020; Woolsey et al., 2021; Vermillion et al., 2021). Similar to humans, SARS-CoV-2 replicates in both the upper and lower respiratory tract tissues of AGMs. SARS-CoV-2 RNA and infectious virus are detected in nasal and throat swabs from AGMs, though more transient in nature compared to the longer duration of viral RNA detection from swabs obtained from humans (Wang et al., 2020).

To determine if systemic GS-441524 could result in SARS-CoV-2 efficacy, we evaluated a 20 mg/kg GS-441524 IV regimen (high dose) for 6 days. This high dose was selected based on the single dose PK data that demonstrated measurable lung tissue TP levels within ~4-fold of those generated by IV 10 mg/kg RDV at 24 h post dose (Table 2). In addition, the GS-441524 exposure from the high dose was projected to be within an attainable dose range for future oral GS-441524 prodrugs. To establish exposure dependent efficacy, an approximately 3-fold lower 7.5 mg/kg IV dose of GS-441524 was administered for 6 days. The GS-441524 treatments were evaluated alongside IV RDV (10/5 mg/kg regimen; a 10 mg/kg loading dose at day 0 followed by maintenance doses of 5 mg/kg on days 1–5). This 10/5 mg/kg RDV regimen has previously demonstrated efficacy in both rhesus and AGM SARS-CoV-2 models (Vermillion et al., 2021; Williamson et al., 2020). Furthermore, this 10/5 mg/kg RDV regimen results in plasma prodrug exposures that are comparable to the clinically approved human 200/100 mg regimen of IV RDV for COVID-19. Confirmation of dose administration throughout the study was monitored by LC/MS/MS analysis of GS-441524 or RDV and its metabolites from inactivated plasma from each animal. Treatment with GS-441524 or RDV was initiated by IV infusion at 8 h post-infection (day 0) and was followed by an additional dose at ~24 h post-infection and then once-daily thereafter. Bronchioalveolar lavage fluid (BALF), nasal swabs, and throat swabs were collected on days 1, 2, 4, and 6 post-infection for quantification of viral load (Fig. 4A). Animals were humanely euthanized on day 6 and upper and lower respiratory tract tissues were harvested for terminal viral load analyses.

Beginning as early as 2 days post-infection, SARS-CoV-2 genomic RNA (gRNA) levels in BALF were significantly reduced by approximately 2 $\log_{10}$ in animals treated with GS-441524 or RDV relative to the vehicle control (Fig. 4B and Table 3). By day 4, all treatment groups, including the lower dose 7.5 mg/kg GS-441524 group, had significant reductions in SARS-CoV-2 gRNA load in BALF, with multiple treatment group animals having gRNA levels below the limit of quantification (BLQ) (Fig. 4B and Table 3). While the majority of animals treated with GS-441524 or RDV did not have quantifiable gRNA levels in BALF on day 6, only 20 mg/kg GS-441524 treatment (in which gRNA was BLQ for all animals), resulted in a statistically significant reduction from the vehicle control.

SARS-CoV-2 sub-genomic RNA (sgRNA) in BALF was only detected in 6 animals (2 from the vehicle group and 4 from the 7.5 mg/kg GS-441524 group) throughout the study. The sgRNA levels in BALF were BLQ at all timepoints for the RDV and 20 mg/kg GS-441524 treatment groups, and the only statistically significant finding was an increase in sgRNA in the 7.5 mg/kg GS-441524 group on day 1 post-infection compared to the vehicle (Table 3). The relevance of this observation is unclear, as it did not correspond with increased gRNA or infectious viral titers, and the low levels of sgRNA in BALF of vehicle control animals limits the utility of this readout for assessing antiviral activity in these

Table 3
SARS-CoV-2 RNA and infectious viral titers in BALF.

DPI	Group	Genomic RNA RT-qPCR			Sub-genomic RNA RT-qPCR			Infectious Virus ($TCID_{50}$)		
		mean log copies/mL (# BLQ)	mean diff.	*p* value	mean log copies/mL (# BLQ)	mean diff.	*p* value	mean log $TCID_{50}$/mL (# BLQ)	mean diff.	*p* value
1	Vehicle	5.99 (0)			2.56 (4)			3.85 (0)		
	20 mg/kg GS-441524	4.86 (0)	−1.13	0.155	1.87 (6)	−0.69	0.0510	0.50 (6)	−3.35	<0.0001
	7.5 mg/kg GS-441524	5.66 (0)	−0.33	>0.999	3.48 (2)	0.92	0.0049	2.02 (2)	−1.83	<0.0001
	10/5 mg/kg RDV	4.90 (0)	−1.09	0.183	1.87 (6)	−0.69	0.0510	1.62 (1)	−2.23	<0.0001
2	Vehicle	5.72 (0)			2.29 (5)			0.90 (4)		
	20 mg/kg GS-441524	3.61 (2)	−2.11	0.001	1.87 (6)	0.42	0.422	0.50 (6)	−0.40	0.582
	7.5 mg/kg GS−441524	5.03 (0)	−0.69	0.691	1.87 (6)	0.42	0.422	0.50 (6)	−0.40	0.582
	10/5 mg/kg RDV	3.83 (1)	−1.89	0.004	1.87 (6)	0.42	0.422	0.72 (4)	−0.18	>0.999
4	Vehicle	5.32 (0)			1.87 (6)			0.50 (6)		
	20 mg/kg GS-441524	2.98 (3)	−2.34	0.0003	1.87 (6)	0	NA	0.50 (6)	0	NA
	7.5 mg/kg GS-441524	3.13 (3)	−2.19	0.0006	1.87 (6)	0	NA	0.50 (6)	0	NA
	10/5 mg/kg RDV	2.81 (4)	−2.51	0.0003	1.87 (6)	0	NA	0.50 (6)	0	NA
6	Vehicle	3.66 (2)			1.87 (6)			–	–	–
	20 mg/kg GS−441524	1.87 (6)	−1.79	0.007	1.87 (6)	0	NA	–	–	–
	7.5 mg/kg GS-441524	2.64 (4)	−1.02	0.234	1.87 (6)	0	NA	–	–	–
	10/5 mg/kg RDV	2.28 (5)	−1.38	0.054	1.87 (6)	0	NA	–	–	–

SARS-CoV-2 genomic RNA copies, sub-genomic RNA copies, and infectious viral titers in BALF collected 1, 2, 4, and 6 days post-infection (DPI) from AGM (n=6/group) dosed daily with IV vehicle, 20 mg/kg GS-441524, 7.5 mg/kg GS-441524, or 10/5 mg/kg RDV.
Samples below the lower limit of quantification for the assay were assigned a value of 1/2 LLOQ for statistical analyses (1.87 for RT-qPCR or 0.5 for $TCID_{50}$). Number of animals BLQ for each group is in parenthesis next to the mean log values.
Group means, mean difference (mean diff.) from vehicle control, and *p* values based on repeated measures two-way ANOVA with Bonferroni post-hoc correction with $p < 0.05$ being considered significant.
Statistics were not performed for analysis in which all animals were BLQ.

samples. Infectious virus, in contrast, was detectable in BALF from all vehicle-treated animals at day 1 post-infection, and all treatment groups demonstrated significant reductions in infectious SARS-CoV-2 titers as compared to vehicle control (Fig. 4C). Treatment of GS-441524 showed a clear dose response on day 1, with the 7.5 mg/kg treatment reducing mean viral titers by 1.8 $\log_{10}$, (with only 1 animal BLQ) while all animals in the 20 mg/kg group had infectious viral titers that were BLQ (>3.35 $\log_{10}$ reduction). By day 2 post-infection, only 2 vehicle animals had quantifiable infectious virus in the BALF, which prevented statistical significance from being achieved despite infectious virus loads that were BLQ for both groups receiving GS-441524. In totality, SARS-CoV-2 antiviral efficacy was observed in BALF samples for all treatment groups, with a dose-dependent response to GS-441524. Moreover, based on these data, treatment with 20 mg/kg GS-441524 demonstrated similar antiviral efficacy to the 10/5 mg/kg RDV regimen.

To investigate the SARS-CoV-2 efficacy of GS-441524 in the upper airway, viral RNA loads and infectious virus titers were quantified from throat and nasal swabs. In RT-qPCR analysis of SARS-CoV-2 gRNA and sgRNA, only sgRNA in the 20 mg/kg GS-441524 group on day 2 from throat swabs was found to be significantly decreased compared to vehicle (Supp. Table 1). In contrast, significant reductions in infectious SARS-CoV-2 titers from throat swabs were observed for both doses of GS-441524 and RDV on day 1 post infection. However, by day 2 post infection, infectious virus from throat swabs became undetectable in all groups (Supp. Fig. 1 and Supp. Table 1). The observed persistence of SARS-CoV-2 RNA following clearance of infectious virus is potentially due to continued sloughing of cells of the upper airway that release non-infectious viral RNA. RT-qPCR from nasal swabs showed no difference in gRNA or sgRNA between vehicle control animals and any treatment group (Supp. Table 2). The sgRNA levels from nasal swabs were below the limit of quantification for most animals and thus $TCID_{50}$ assays were not performed on these samples as they would likely be below the limit of detection.

Terminal respiratory tissue homogenates from the lung (upper, middle, and lower), trachea, as well as lower and mainstem bronchus were assessed for SARS-CoV-2 loads. The most pronounced antiviral effect for all compounds was observed in the lower lung in which both doses of GS-441524 and RDV significantly reduced SARS-CoV-2 infectious virus and sgRNA (Fig. 5A and B and Table 4). While all treatments also reduced average gRNA loads in the lower lung by > 2 $\log_{10}$, only GS-441524 at 20 mg/kg achieved statistical significance (Fig. 5C and Table 4). 20 mg/kg GS-441524 treatments also significantly reduced SARS-CoV-2 infectious virus titers in the mainstem and lower bronchus (Fig. 5D and E) as well as gRNA and sgRNA levels in the upper lung (Supp. Fig. 2 and Table 4). Viral RNA and infectious viral titers in the middle lung and trachea were similar to vehicle for all treatment groups (Supp. Fig. 2 and Table 4). Taken together, the tissue analyses suggest that GS-441524 at 20 mg/kg was the most consistently efficacious treatment for limiting SARS-CoV-2 viral load among the various treatment arms.

All treatments were well tolerated by the animals for the duration of the study, with no remarkable changes in body weights. Samples for

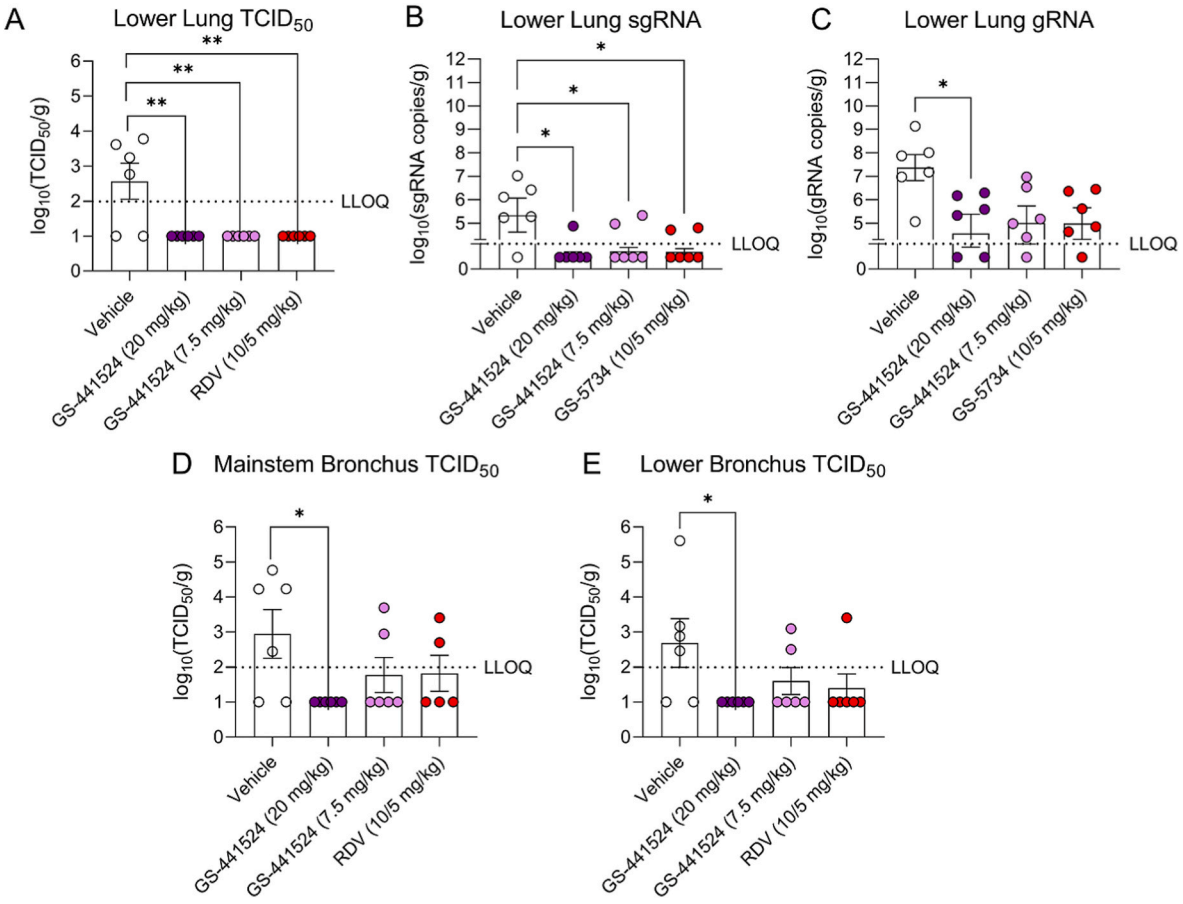

Fig. 5. 20 mg/kg GS-441524 inhibits SARS-CoV-2 in respiratory tissue. AGM (n = 6/group) were inoculated with SARS-CoV-2 and treated daily with IV GS-441524 at 20 mg/kg (dark purple symbols) or 7.5 mg/kg IV (light purple symbols), with RDV at 10/5 mg/kg (red symbols) or vehicle (open symbols). At 6 days post-infection, SARS-CoV-2 infectious virus (A), sgRNA (B), and gRNA (C) from the lower lung were quantified by $TCID_{50}$ or RT-qPCR. Infectious virus ($TCID_{50}$) loads were also assessed at 6 days post-infection from mainstem (D) and lower (E) bronchial tissue. Samples below the lower limit of quantification (LLOQ, dotted lines) for the assay were assigned a value of 1/2 LLOQ for statistical analyses. Data from tissue samples were analyzed using a one-way ANOVA with Bonferroni post-hoc correction compared to vehicle. A corrected $p < 0.05$ was considered significant with $^{*}p < 0.05$, $^{**}p < 0.01$.

Table 4
SARS-CoV-2 RNA and infectious viral titers from respiratory tissue.

Tissue	Group	Genomic RNA RT-qPCR			Sub-genomic RNA RT-qPCR			Infectious Virus ($TCID_{50}$)		
		mean log copies/mL (# BLQ)	mean diff.	*p* value	mean log copies/mL (# BLQ)	mean diff.	*p* value	mean log $TCID_{50}$/mL (# BLQ)	mean diff.	*p* value
Lower Bronchus	Vehicle	7.61 (0)			5.88 (0)			2.68 (2)		
	20 mg/kg GS-441524	5.77 (0)	−1.84	0.117	2.53 (5)	−3.35	0.0006	1.00 (6)	−1.68	0.0439
	7.5 mg/kg GS-441524	6.53 (1)	−1.08	0.623	5.04 (1)	−0.84	0.807	1.60 (4)	−1.08	0.302
	10/5 mg/kg RDV	7.47 (0)	−0.14	>0.999	5.75 (0)	−0.13	>0.999	1.40 (5)	−1.28	0.166
Mainstem Bronchus	Vehicle	7.79 (0)			6.16 (0)			2.94 (2)		
	20 mg/kg GS-441524	4.45 (2)	−3.34	0.0046	2.98 (4)	−3.18	0.0241	1.00 (6)	−1.94	0.0330
	7.5 mg/kg GS-441524	6.39 (0)	−1.40	0.415	3.25 (4)	−2.91	0.0416	1.77 (4)	−1.17	0.317
	10/5 mg/kg RDV	7.07 (0)	−0.72	>0.999	4.14 (3)	−2.02	0.229	1.82 (4)	−1.12	0.411
Lower Lung	Vehicle	7.37 (0)			5.35 (1)			2.57 (2)		
	20 mg/kg GS-441524	4.56 (2)	−2.81	0.0304	2.48 (5)	−2.87	0.0115	1.00 (6)	−1.57	0.0011
	7.5 mg/kg GS-441524	5.01 (1)	−2.36	0.0812	3.05 (4)	−2.30	0.0494	1.00 (6)	−1.57	0.0011
	10/5 mg/kg RDV	4.99 (1)	−2.38	0.0770	2.92 (4)	−2.43	0.0358	1.00 (6)	−1.57	0.0011
Middle Lung	Vehicle	7.53 (0)			4.95 (2)			–	–	–
	20 mg/kg GS-441524	5.76 (1)	−1.77	0.373	3.71 (3)	−1.24	0.949	–	–	–
	7.5 mg/kg GS-441524	6.14 (1)	−1.39	0.672	4.38 (2)	−0.57	>0.999	–	–	–
	10/5 mg/kg RDV	6.13 (0)	−1.40	0.657	3.31 (4)	−1.64	0.574	–	–	–
Upper Lung	Vehicle	7.04 (0)			4.85 (1)			–	–	–
	20 mg/kg GS-441524	3.55 (3)	−3.49	0.0019	2.00 (6)	−2.85	0.0054	–	–	–
	7.5 mg/kg GS-441524	6.23 (0)	−0.81	>0.999	3.67 (3)	−1.18	0.460	–	–	–
	10/5 mg/kg RDV	5.03 (1)	−2.01	0.0923	2.51 (5)	−2.34	0.0232	–	–	–
Trachea	Vehicle	7.00 (0)			3.26 (4)			–	–	–
	20 mg/kg GS-441524	5.22 (1)	−1.78	0.169	2.66 (5)	−0.60	>0.999	–	–	–
	7.5 mg/kg GS−441524	6.04 (0)	−0.96	0.866	3.15 (4)	−0.11	>0.999	–	–	–
	10/5 mg/kg RDV	6.93 (0)	−0.07	>0.999	4.36 (2)	1.10	0.914	–	–	–

SARS-CoV-2 genomic RNA copies, sub-genomic RNA copies, and infectious viral titers from respiratory tissue (lung, bronchus, trachea) harvested at 6 days post infection (DPI) from AGM (n=6/group) dosed daily with IV vehicle, 20 mg/kg GS-441524, 7.5 mg/kg GS-441524, or 10/5 mg/kg RDV.
Samples below the lower limit of quantification for the assay were assigned a value of 1/2 LLOQ for statistical analyses (1.87 for RT-qPCR or 1.0 for $TCID_{50}$).
$TCID_{50}$ was not performed on tissue samples with mean sgRNA levels below 5.0 logs.
Group means, mean difference (mean diff.) from vehicle control, and *p* values based on one-way ANOVA with Bonferroni post-hoc correction, $p < 0.05$ is considered significant.

clinical pathology analyses (hematology, serum chemistry, and coagulation) were assessed pre-dose, day 3, and day 6 post-infection. No treatment related changes in hematology or coagulation were observed, and all clinical chemistry parameters remained within normal reference intervals.

3. Discussion and conclusions

As the COVID-19 pandemic continues and new variants emerge, there remains an urgent need to identify and develop effective therapies with broad-spectrum anti-coronavirus efficacy. RDV (VEKLURY®) was the first approved therapy for patients with COVID-19 in the United States, Japan, the European Union, and other countries. Both RDV and its parent nucleoside, GS-441524, retain *in vitro* potency across all recently emergent variants of concern and variants of interest (Pitts et al., 2022). In addition to SARS-CoV-2 antiviral activity, RDV has previously demonstrated potent activity against other epidemic coronaviruses, such as SARS-CoV and MERS-CoV (Sheahan et al., 2017, 2020; Agostini et al., 2018). GS-441524, meanwhile has been found to be highly efficacious both *in vitro* and *in vivo* against mouse hepatitis virus (Li et al., 2021b) and feline infectious peritonitis virus (Murphy et al., 2018; Pedersen et al., 2019), two zoonotic coronaviruses. In totality, these results highlight the broad-spectrum coronavirus activity of GS-441524 and RDV.

RDV is efficiently metabolized to the pharmacologically active TP within lung cells *in vitro* and *in vivo* leading to high TP levels in non-human primates at 24 h post infusion despite its short plasma half-life. In contrast, GS-441524 is less efficient in TP loading within lung cells both *in vitro* and *in vivo*. We hypothesized that higher plasma exposures of GS-441524 may be able to overcome its metabolic limitations and generate sufficient TP in infected cells of the lung to support SARS-CoV-2 antiviral efficacy. In transgenic mice, it was demonstrated that intragastric injection GS-441524 yielded high plasma exposures of GS-441524 and resulted in SARS-CoV-2 efficacy (Li et al., 2021b). More recent studies have shown that sufficient systemic levels of GS-441524 can be achieved in ferrets and mice through oral delivery of GS-441524 prodrugs, resulting in robust *in vivo* efficacy against SARS-CoV-2 (Cox et al., 2021; Schafer et al., 2022). In this study, we sought to investigate whether systemic exposures of GS-441524 delivered by IV would result in SARS-CoV-2 efficacy in a non-human primate

model of SARS-CoV-2 infection and to determine the systemic exposure levels of GS-441524 required for a significant reduction in viral load. The demonstration of SARS-CoV-2 efficacy and the elucidation of the required systemic GS-441524 levels support the discovery and development of orally bioavailable prodrugs capable of efficient systemic delivery of GS-441524.

Alveolar Type II (AT2 or pneumocytes) cells and ciliated bronchial epithelial cells both express ACE2 and TMPRSS2 genes at relatively high levels, suggesting they are target cells for SARS-CoV-2 replication (Sungnak et al., 2020). In this context, we tested antiviral activity and monitor TP formation from GS-441524 and RDV in the physiologically relevant NHBE cells (undifferentiated precursors to the ciliated epithelial cells) and EpiAlveolar cells (3D culture containing Alveolar Type I and Type II cells). In both EpiAlveolar and NHBE cells, GS-441524 was less potent against SARS-CoV-2 and produced lower intracellular TP levels when compared to RDV. This correlation between TP level and SARS-CoV-2 antiviral potency is consistent with previous findings in other cell types such as human airway epithelial (HAE) cultures and Calu-3 (Pruijssers et al., 2020), as well as with results reported for comparative RSV antiviral potency in NHBE cultures (Mackman et al., 2021). In contrast, RDV and GS-441524 were shown to have similar SARS-CoV-2 potencies in Vero E6 cells, derived from AGM kidney cells that were found to produce low TP levels from both drugs (Pruijssers et al., 2020). To determine if the observed reduction in RDV metabolism to the active TP in Vero E6 cells was a species-specific effect in AGM cells, we performed a metabolism study of RDV and GS-441524 in AGM bronchial epithelial cells. In line with our findings in NHBE cells, RDV produced 11.5-fold more TP than GS-441524 in AGM bronchial epithelial cells, indicating the antiviral and metabolic phenotype in Vero E6 is not simply due to species differences between AGM and humans.

The differential *in vitro* metabolism results from AGM bronchial epithelial cells that showed more efficient intracellular TP formation following incubation with RDV compared to GS-441524 were consistent with those obtained from subsequent *in vivo* single-dose PK studies. Following IV administration in AGM, GS-441524 given at 20 mg/kg yielded plasma GS-441524 C_{max} and 24 h AUC values that were 70- and 16-fold higher, respectively, compared to those obtained following RDV administration at 10 mg/kg. However, lower lung tissue collected at 24 h showed measurable levels of TP that were 4-fold lower than those observed in animals that received 10 mg/kg RDV. On a molar basis, the GS-441524 dose of 20 mg/kg is 4-fold higher than that of 10 mg/kg RDV, highlighting the 16-fold difference in efficiency at generating TP in lower lung of AGMs, consistent with the 15-fold observation previously reported for cynomolgus monkey (Mackman et al., 2021). There are several key conclusions from these pharmacokinetic studies that support the design of the AGM efficacy study. First, the more sustained but relatively low systemic exposures of GS-441524 observed following IV RDV administration does not meaningfully contribute to the measured lung tissue TP levels at 24 h. Second, the superior tissue TP generation from IV RDV dosing is likely the result of this prodrug's ability to rapidly distribute into and activate within lung tissues, in spite of its short plasma half-life, combined with a prolonged TP half-life of ~14 h. Lastly, increasing the exposure of GS-441524 can overcome the limited metabolism and generate measurable tissue TP levels that may provide efficacy. The AGM PK results presented here and the previously reported cynomolgus PK (Mackman et al., 2021) fully support the clinical development of the prodrug RDV over GS-441524 for IV delivered therapy.

In the AGM SARS-CoV-2 efficacy study, we evaluated high systemic exposures of GS-441524 and compared the resulting efficacy to that of IV RDV. We noted that all 3 treatment regimens (20 mg/kg GS-441524, 7.5 mg/kg GS-441524, and 10/5 mg/kg RDV) were well tolerated in animals with no remarkable safety signals observed in coagulation, clinical chemistry, and hematologic markers. Although the safety profile of GS-4415124 has not been fully evaluated, additional *in vitro* screening has shown no off-target activity against a panel of targets consisting of receptors, ion channels, and transporters at 10 μM, no significant inhibition of the hERG channel at 30 μM, and no mutagenic activity in an Ames bacterial mutation assay (unpublished data). Further, extensive profiling in cellular and biochemical assays with GS-441524 showed a low potential for cytotoxicity and mitochondria-related toxicity (30).

All treatment regimens were observed to be efficacious based on multiple analyses from the BALF and respiratory tissue samples. The 20 mg/kg GS-441524 group consistently resulted in greater reductions of both SARS-CoV-2 infectious titers as well as genomic and sub-genomic viral RNA loads compared to the 7.5 mg/kg GS-441524 group. While all regimens were efficacious in reducing infectious viral titers in the BALF and lower lung, only the 20 mg/kg GS-441524 regimen also reduced infectious viral loads in the conducting airways (i.e. mainstem and lower bronchus). In totality, the 20 mg/kg GS-441524 IV dose was more consistently efficacious in reducing viral load than the 7.5 mg/kg dose, illustrating a dose response to GS-441524 exposure. Importantly, 20 mg/kg IV GS-441524 had at least equivalent efficacy to the standard IV regimen of RDV and was the most effective treatment in reducing infectious viral loads in terminal respiratory tissues.

The strong efficacy results with GS-441524 IV infusion at the 20 mg/kg dose are somewhat unexpected considering the observed lower levels of TP formed at 24 h in the lower lung compared to IV RDV in the single-dose AGM PK study. The most likely explanation is that the TP levels measured in lower lung tissue at a discrete time point are a poor indicator of efficacy, potentially due to intracellular RDV metabolism being more ubiquitous than GS-441524 leading to TP formation in cells which are non-permissive for SARS-CoV-2 infection (Yan and Muller, 2020). Since the PK tissue sampling includes TP derived from all cell types found in the lower lung, it is possible that TP levels in SARS-CoV-2 permissive cells from GS-441524 and RDV are more similar than the analysis of whole lung homogenate suggests. Further, the TP levels in lung tissue were measured at a single time point of 24 h post-dose which may not be representative of the TP levels across the whole 6-day dosing interval. Regardless, additional studies are required to better understand the biomarkers which are predictive of antiviral efficacy in the SARS-CoV-2 AGM model.

In summary, GS-441524, the parent nucleoside of RDV, is efficacious in an AGM model of SARS-CoV-2 infection when sufficiently high systemic exposures of GS-441524 are achieved. The circulating levels of GS-441524 required for efficacy comparable with IV RDV in the AGM model are significantly higher than those observed in humans following IV administration of the approved RDV dose, strongly indicating that the observed clinical efficacy of RDV across the COVID-19 disease spectrum is driven by the intact RDV exposures rather than by the systemic levels of GS-441524 generated from RDV, contrary to previous suggestions (Yan and Muller, 2020). For this reason, RDV is the appropriate choice for IV administration, but oral antivirals are still be the preferred treatment route, especially in an outpatient settings. While studies in rodents and dogs have demonstrated good oral bioavailability of GS-441524 (Wang et al., 2022), pharmacokinetic profiling in all non-human primate species found the oral bioavailability of GS-441524 to be low (<10%), suggesting that the oral delivery of GS-441524 itself might still require relatively high doses or more frequent administration to achieve the exposures required for clinical efficacy. Therefore, oral GS-441524 prodrugs that increase oral bioavailability and systemic exposures of GS-441524 are worth exploring as candidate outpatient therapies for COVID-19 patients to prevent the progression of disease and hospitalization.

Funding

These studies were fully funded by Gilead Sciences, Inc. Work conducted at the University of Texas Medical Branch (UTMB) was done under a Gilead-UTMB funded research agreement.

Declaration of competing interest

The authors declare the following financial interests/personal relationships which may be considered as potential competing interests: The authors affiliated with Gilead Sciences, Inc. are employees of the company and may own company stock. These studies were fully funded by Gilead Sciences, Inc. Work conducted at the University of Texas Medical Branch (UTMB) was done under a Gilead-UTMB funded research agreement.

Appendix A. Supplementary data

Supplementary data to this article can be found online at https://doi.org/10.1016/j.antiviral.2022.105329.

References

Agostini, M.L., Andres, E.L., Sims, A.C., Graham, R.L., Sheahan, T.P., Lu, X., Smith, E.C., Case, J.B., Feng, J.Y., Jordan, R., Ray, A.S., Cihlar, T., Siegel, D., Mackman, R.L., Clarke, M.O., Baric, R.S., Denison, M.R., 2018. Coronavirus susceptibility to the antiviral remdesivir (GS-5734) is mediated by the viral polymerase and the proofreading exoribonuclease. mBio 9.

Cox, R.M., Wolf, J.D., Lieber, C.M., Sourimant, J., Lin, M.J., Babusis, D., DuPont, V., Chan, J., Barrett, K.T., Lye, D., Kalla, R., Chun, K., Mackman, R.L., Ye, C., Cihlar, T., Martinez-Sobrido, L., Greninger, A.L., Bilello, J.P., Plemper, R.K., 2021. Oral prodrug of remdesivir parent GS-441524 is efficacious against SARS-CoV-2 in ferrets. Nat. Commun. 12, 6415.

Cross, R.W., Agans, K.N., Prasad, A.N., Borisevich, V., Woolsey, C., Deer, D.J., Dobias, N. S., Geisbert, J.B., Fenton, K.A., Geisbert, T.W., 2020. Intranasal exposure of African green monkeys to SARS-CoV-2 results in acute phase pneumonia with shedding and lung injury still present in the early convalescence phase. Virol. J. 17, 125.

Gordon, C.J., Tchesnokov, E.P., Woolner, E., Perry, J.K., Feng, J.Y., Porter, D.P., Gotte, M., 2020. Remdesivir is a direct-acting antiviral that inhibits RNA-dependent RNA polymerase from severe acute respiratory syndrome coronavirus 2 with high potency. J. Biol. Chem. 295, 6785–6797.

Humeniuk, R., Mathias, A., Cao, H., Osinusi, A., Shen, G., Chng, E., Ling, J., Vu, A., German, P., 2020. Safety, tolerability, and pharmacokinetics of remdesivir, an antiviral for treatment of COVID-19, in healthy subjects. Clin. Transl. Sci. 13, 896–906.

Kokic, G., Hillen, H.S., Tegunov, D., Dienemann, C., Seitz, F., Schmitzova, J., Farnung, L., Siewert, A., Hobartner, C., Cramer, P., 2021. Mechanism of SARS-CoV-2 polymerase stalling by remdesivir. Nat. Commun. 12, 279.

Li, R., Liclican, A., Xu, Y., Pitts, J., Niu, C., Zhang, J., Kim, C., Zhao, X., Soohoo, D., Babusis, D., Yue, Q., Ma, B., Murray, B.P., Subramanian, R., Xie, X., Zou, J., Bilello, J. P., Li, L., Schultz, B.E., Sakowicz, R., Smith, B.J., Shi, P.Y., Murakami, E., Feng, J.Y., 2021a. Key metabolic enzymes involved in remdesivir activation in human lung cells. Antimicrob. Agents Chemother. https://doi.org/10.1128/AAC.00602-21: AAC0060221.

Li, Y., Cao, L., Li, G., Cong, F., Li, Y., Sun, J., Luo, Y., Chen, G., Li, G., Wang, P., Xing, F., Ji, Y., Zhao, J., Zhang, Y., Guo, D., Zhang, X., 2021b. Remdesivir metabolite GS-441524 effectively inhibits SARS-CoV-2 infection in mouse models. J. Med. Chem. https://doi.org/10.1021/acs.jmedchem.0c01929.

Mackman, R.L., Hui, H.C., Perron, M., Murakami, E., Palmiotti, C., Lee, G., Stray, K., Zhang, L., Goyal, B., Chun, K., Byun, D., Siegel, D., Simonovich, S., Du Pont, V., Pitts, J., Babusis, D., Vijjapurapu, A., Lu, X., Kim, C., Zhao, X., Chan, J., Ma, B., Lye, D., Vandersteen, A., Wortman, S., Barrett, K.T., Toteva, M., Jordan, R., Subramanian, R., Bilello, J.P., Cihlar, T., 2021. Prodrugs of a 1'-CN-4-Aza-7,9-dideazaadenosine C-nucleoside leading to the discovery of remdesivir (GS-5734) as a potent inhibitor of respiratory syncytial virus with efficacy in the african green monkey model of RSV. J. Med. Chem. 64, 5001–5017.

Menachery, V.D., Yount Jr., B.L., Sims, A.C., Debbink, K., Agnihothram, S.S., Gralinski, L. E., Graham, R.L., Scobey, T., Plante, J.A., Royal, S.R., Swanstrom, J., Sheahan, T.P., Pickles, R.J., Corti, D., Randell, S.H., Lanzavecchia, A., Marasco, W.A., Baric, R.S., 2016. SARS-like WIV1-CoV poised for human emergence. Proc. Natl. Acad. Sci. U. S. A. 113, 3048–3053.

Murphy, B.G., Perron, M., Murakami, E., Bauer, K., Park, Y., Eckstrand, C., Liepnieks, M., Pedersen, N.C., 2018. The nucleoside analog GS-441524 strongly inhibits feline infectious peritonitis (FIP) virus in tissue culture and experimental cat infection studies. Vet. Microbiol. 219, 226–233.

Pedersen, N.C., Perron, M., Bannasch, M., Montgomery, E., Murakami, E., Liepnieks, M., Liu, H., 2019. Efficacy and safety of the nucleoside analog GS-441524 for treatment of cats with naturally occurring feline infectious peritonitis. J. Feline Med. Surg. 21, 271–281.

Pitts, J., Li, J., Perry, J.K., Du Pont, V., Riola, N., Rodriguez, L., Lu, X., Kurhade, C., Xie, X., Camus, G., Manhas, S., Martin, R.W., Shi, P.Y., Cihlar, T., Porter, D.P., Mo, H., Maiorova, E., Bilello, J.P., 2022. Remdesivir and GS-441524 retain antiviral activity against Delta, Omicron, and other emergent SARS-CoV-2 variants. Antimicrob. Agents Chemother. https://doi.org/10.1101/2022.02.09.479840.

Pruijssers, A.J., George, A.S., Schafer, A., Leist, S.R., Gralinksi, L.E., Dinnon 3rd, K.H., Yount, B.L., Agostini, M.L., Stevens, L.J., Chappell, J.D., Lu, X., Hughes, T.M., Gully, K., Martinez, D.R., Brown, A.J., Graham, R.L., Perry, J.K., Du Pont, V., Pitts, J., Ma, B., Babusis, D., Murakami, E., Feng, J.Y., Bilello, J.P., Porter, D.P., Cihlar, T., Baric, R.S., Denison, M.R., Sheahan, T.P., 2020. Remdesivir inhibits SARS-CoV-2 in human lung cells and chimeric SARS-CoV expressing the SARS-CoV-2 RNA polymerase in mice. Cell Rep. 32, 107940.

Schafer, A., Martinez, D.R., Won, J.J., Moreira, F.R., Brown, A.J., Gully, K.L., Kalla, R., Chun, K., Du Pont, V., Babusis, D., Tang, J., Murakami, E., Subramanian, R., Barrett, K.T., Bleier, B.J., Bannister, R., Feng, J.Y., Bilello, J.P., Cihlar, T., Mackman, R.L., Montgomery, S.A., Baric, R.S., Sheahan, T.P., 2022. Therapeutic efficacy of an oral nucleoside analog of remdesivir against SARS-CoV-2 pathogenesis in mice. Sci. Transl. Med. https://doi.org/10.1126/scitranslmed.abm3410. https://www.science.org/doi/10.1126/scitranslmed.abm3410.

Sheahan, T., Rockx, B., Donaldson, E., Corti, D., Baric, R., 2008. Pathways of cross-species transmission of synthetically reconstructed zoonotic severe acute respiratory syndrome coronavirus. J. Virol. 82, 8721–8732.

Sheahan, T.P., Sims, A.C., Graham, R.L., Menachery, V.D., Gralinski, L.E., Case, J.B., Leist, S.R., Pyrc, K., Feng, J.Y., Trantcheva, I., Bannister, R., Park, Y., Babusis, D., Clarke, M.O., Mackman, R.L., Spahn, J.E., Palmiotti, C.A., Siegel, D., Ray, A.S., Cihlar, T., Jordan, R., Denison, M.R., Baric, R.S., 2017. Broad-spectrum antiviral GS-5734 inhibits both epidemic and zoonotic coronaviruses. Sci. Transl. Med. 9.

Sheahan, T.P., Sims, A.C., Leist, S.R., Schafer, A., Won, J., Brown, A.J., Montgomery, S. A., Hogg, A., Babusis, D., Clarke, M.O., Spahn, J.E., Bauer, L., Sellers, S., Porter, D., Feng, J.Y., Cihlar, T., Jordan, R., Denison, M.R., Baric, R.S., 2020. Comparative therapeutic efficacy of remdesivir and combination lopinavir, ritonavir, and interferon beta against MERS-CoV. Nat. Commun. 11, 222.

Sungnak, W., Huang, N., Becavin, C., Berg, M., Queen, R., Litvinukova, M., Talavera-Lopez, C., Maatz, H., Reichart, D., Sampaziotis, F., Worlock, K.B., Yoshida, M., Barnes, J.L., Network, H.C.A.L.B., 2020. SARS-CoV-2 entry factors are highly expressed in nasal epithelial cells together with innate immune genes. Nat. Med. 26, 681–687.

Tchesnokov, E.P., Gordon, C.J., Woolner, E., Kocinkova, D., Perry, J.K., Feng, J.Y., Porter, D.P., Gotte, M., 2020. Template-dependent inhibition of coronavirus RNA-dependent RNA polymerase by remdesivir reveals a second mechanism of action. J. Biol. Chem. 295, 16156–16165.

Van Rompay, A.R., Johansson, M., Karlsson, A., 2000. Phosphorylation of nucleosides and nucleoside analogs by mammalian nucleoside monophosphate kinases. Pharmacol. Ther. 87, 189–198.

Vermillion, M.S., Murakami, E., Ma, B., Pitts, J., Tomkinson, A., Rautiola, D., Babusis, D., Irshad, H., Siegel, D., Kim, C., Zhao, X., Niu, C., Yang, J., Gigliotti, A., Kadrichu, N., Bilello, J.P., Ellis, S., Bannister, R., Subramanian, R., Smith, B., Mackman, R.L., Lee, W.A., Kuehl, P.J., Hartke, J., Cihlar, T., Porter, D.P., 2021. Inhaled remdesivir reduces viral burden in a nonhuman primate model of SARS-CoV-2 infection. Sci. Transl. Med. 14 (633), eabl828 https://doi.org/10.1126/scitranslmed.abl8282.

Wang, K., Zhang, X., Sun, J., Ye, J., Wang, F., Hua, J., Zhang, H., Shi, T., Li, Q., Wu, X., 2020. Differences of severe acute respiratory syndrome coronavirus 2 shedding duration in sputum and nasopharyngeal swab specimens among adult inpatients with coronavirus disease 2019. Chest 158, 1876–1884.

Wang, A.Q., Hagen, N.R., Padilha, E.C., Yang, M., Shah, P., Chen, C.Z., Huang, W., Terse, P., Sanderson, P., Zheng, W., Xu, X., 2022. Preclinical pharmacokinetics and in vitro properties of GS-441524, A potential oral drug candidate for COVID-19 treatment. bioRxiv doi. https://doi.org/10.1101/2022.02.07.478848.

Williamson, B.N., Feldmann, F., Schwarz, B., Meade-White, K., Porter, D.P., Schulz, J., van Doremalen, N., Leighton, I., Yinda, C.K., Perez-Perez, L., Okumura, A., Lovaglio, J., Hanley, P.W., Saturday, G., Bosio, C.M., Anzick, S., Barbian, K., Cihlar, T., Martens, C., Scott, D.P., Munster, V.J., de Wit, E., 2020. Clinical benefit of remdesivir in rhesus macaques infected with SARS-CoV-2. Nature 585, 273–276.

Woolsey, C., Borisevich, V., Prasad, A.N., Agans, K.N., Deer, D.J., Dobias, N.S., Heymann, J.C., Foster, S.L., Levine, C.B., Medina, L., Melody, K., Geisbert, J.B., Fenton, K.A., Geisbert, T.W., Cross, R.W., 2021. Establishment of an African green monkey model for COVID-19 and protection against re-infection. Nat. Immunol. 22, 86–98.

Xie, J., Wang, Z., 2021. Can remdesivir and its parent nucleoside GS-441524 be potential oral drugs? An in vitro and in vivo DMPK assessment. Acta Pharm. Sin. B 11, 1607–1616.

Xie, X., Muruato, A.E., Zhang, X., Lokugamage, K.G., Fontes-Garfias, C.R., Zou, J., Liu, J., Ren, P., Balakrishnan, M., Cihlar, T., Tseng, C.K., Makino, S., Menachery, V.D., Bilello, J.P., Shi, P.Y., 2020. A nanoluciferase SARS-CoV-2 for rapid neutralization testing and screening of anti-infective drugs for COVID-19. Nat. Commun. 11, 5214.

Yan, V.C., Muller, F.L., 2020. Advantages of the parent nucleoside GS-441524 over remdesivir for covid-19 treatment. ACS Med. Chem. Lett. 11, 1361–1366.